

## **Behaviour of Continuous Concrete Deep Beams Reinforced with GFRP Headed Bars**

Ahmed Mohamed<sup>1</sup>, Ehab El-Salakawy<sup>1</sup>

<sup>1</sup> *Department of Civil Engineering, University of Manitoba, Winnipeg, MB, Canada*

### **Abstract**

Reinforced concrete (RC) continuous deep beams are one of the common components in the superstructure of bridges and multistory buildings. Deep beams have higher load capacity compared to slender beams. They are characterized by their small shear span-to-depth ratio ( $< 2.0$ ) and they are usually designed using the Strut-and-Tie Model (STM). Recently, fibre-reinforced polymer (FRP) bars have been used as an alternative to steel bars to overcome the corrosion problems. However, due to its linear-elastic behaviour and relatively low modulus of elasticity compared to steel, glass FRP (GFRP)-RC continuous deep beams would be susceptible to deeper and wider cracks as well as lack of ability to redistribute stresses, which will adversely affect the capacity of such beams. In this study, three large-scale continuous RC deep beams reinforced with GFRP headed-end bars were constructed and tested up to failure. The specimens had a rectangular-section of 250×590 mm and a length of 3,500 mm. The main variable was top longitudinal reinforcement ratio, which varied between 1.2, 1.0, and 0.8%. The test results confirmed the formation of the strut-and-tie model. Also, it showed that decreasing the top longitudinal reinforcement ratio led to decreasing the load capacity of such beams.

**Keywords:** Continuous deep beams, Glass fiber-reinforced polymers (GFRP), Headed-end bars, Shear span-to-depth ratio, Shear strength, Strut-and-tie model.

**Corresponding author's email:** [Ehab.El-Salakawy@umanitoba.ca](mailto:Ehab.El-Salakawy@umanitoba.ca)

## Introduction

For over a century, the behaviour of steel-RC structures has been investigated in many research studies. Deep beams are commonly used in structural applications such as bridges and high-rise buildings, as they are well known with their relatively higher load capacity compared to slender beams. These types of structures are exposed to harsh environment specially in North America which, over time, can cause severe deterioration due to the corrosion problems. Thus, the use of fibre-reinforced polymers (FRP) bars became more common in the last two decades as they are noncorrosive materials [1,2].

It is well established that in deep beams, which have a shear span-to-depth ratio ( $a/d$ ) less than 2.0 [3,4], after the formation of the diagonal crack, internal forces are reoriented, as the load is transferred from the load point to the supports by inclined concrete struts forming the arch action. In the meantime, the longitudinal reinforcement work as tie which holds the base of the arch together. Such load transfer mechanism is named arch action or strut-and-tie model (STM).

The shear behaviour of the glass FRP (GFRP)-RC beams is similar to that of steel-RC beams; however, GFRP-RC beams have a lower shear capacity due the relatively low modulus of elasticity of GFRP with respect to steel, which will result in wider and deeper cracks that adversely affect the contribution of the uncracked concrete and the aggregate interlock [5]. Using GFRP in RC deep beams will results in decreasing the efficiency factor of the strut due to the wider and deeper cracks that propagate in the GFRP-RC members, which in turn will adversely affect the capacity of the strut and tie model.

Moreover, the behaviour of continuous deep beams is different from that of simply-supported ones, due to the presence of higher shear force and bending moment at the same region above intermediate supports, in addition to the linear-elastic behaviour, which will adversely affect the efficiency of the interior strut and the redistribution of stresses. Many researches have been conducted to investigate the shear behaviour of steel-RC simply-supported and continuous concrete deep beams [6-9]. This paper aims to investigate the shear behaviour of continuous deep beams reinforced with GFRP that do not contain any web reinforcement.

## Experimental Program

### Test specimens

Three large-scale concrete deep beams reinforced with GFRP were constructed and tested to failure. All specimens had a rectangular cross section of 250 x 590 mm,  $a/d$  of 1.0 and bottom longitudinal reinforcement ratio,  $\rho_{bot}$ , of 1.0% and an overall length of 3,500 mm. The top longitudinal reinforcement ratio,  $\rho_{top}$ , varied between 1.2, 1.0 and 0.8%. The test specimens were labelled based on the top longitudinal reinforcement ratio. For example, Specimen B 1.2 is the beam specimen that has  $\rho_{top} = 1.2\%$ . Table 1 lists The details of the specimens.

Table 1:Details of test specimens

| Beam ID | $d^*$ (mm) | $a^{**}$ (mm) | $a/d$ | $f_c'$ (MPa) | $\rho_{top}$ (%) | $\rho_{bot}$ (%) |
|---------|------------|---------------|-------|--------------|------------------|------------------|
| B 1.2   | 509        | 520           | 1.0   | 49           | 1.2              | 1.0              |
| B 1.0   | 509        | 520           | 1.0   | 48           | 1.0              | 1.0              |
| B 0.8   | 509        | 520           | 1.0   | 49           | 0.8              | 1.0              |

\*  $d$  is the effective depth

\*\*  $a$  is the clear shear span

## Material properties

Table 2 shows the properties of the used GFRP reinforcing bars. The concrete compressive and tensile strengths were determined on the day of testing according to ASTM C39 (ASTM 2012a) and ASTM C 496 (ASTM 2017). The concrete strengths are listed in Table 1.

Table 2: Mechanical properties of GFRP bars

| Bar No. | Diameter (mm) | Area (mm <sup>2</sup> ) | Tensile Strength (MPa) | Modulus of Elasticity (GPa) | Ultimate Strain (%) |
|---------|---------------|-------------------------|------------------------|-----------------------------|---------------------|
| 15M     | 15.9 (19.2)*  | 198 (291)*              | 1,184                  | 62.6                        | 1.89                |
| 20M     | 19.0 (22.4)*  | 285 (394)*              | 1,105                  | 63.7                        | 1.73                |

\* Effective diameter and cross-sectional area including sand coating.

## Test setup and instrumentation

Three specimens were tested under a monotonic load acting at the middle of each span. Through a spreader stiff beam. Bearing plates were 150×250×500 mm at the exterior supports and 200×250×150 mm at middle support and loading point. To capture the strain profile in the reinforcement, fourteen strain gauges were attached to the reinforcement. Also, six linear variable displacement transducers (LVDTs) were installed. In addition, seven PI-gauges were installed to capture the propagation and widening of cracks.

Figure 1 shows a schematic drawing of the test setup.

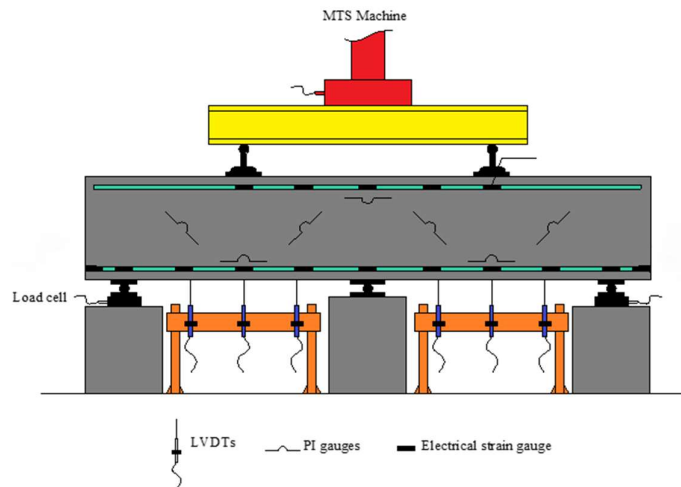


Figure 1: Test setup and instrumentation

## Test Results and Discussion

### Crack pattern and failure mechanism

In initial stages of loading, flexural cracks started propagating in the hogging zone above middle support then in the sagging zone. Such cracks propagated vertically with further loading. At higher loads, flexural shear cracks developed in the interior shear spans in the vicinity of the middle support, then in the exterior shear spans. With further loading, a diagonal shear crack developed between the loading points and the middle support. The width of the diagonal crack kept increasing with applying more load until failure. Figure 2 shows crack

pattern near failure of test beams. Failure of diagonal compression strut in the region between the loading and supporting plates occurred in all specimens. Specimen B1.2 exhibited a shear compression failure. On the other hand, specimens B1.0 and B0.8 had a compression strut failure, as shown in Figure 3.

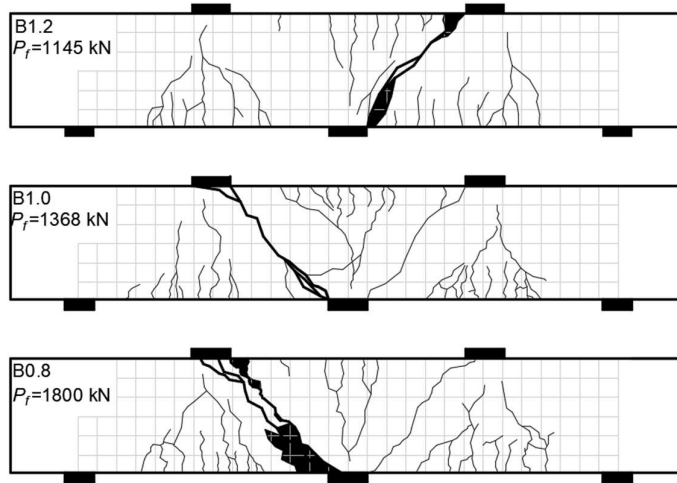


Figure 2: Crack pattern near failure of test beams

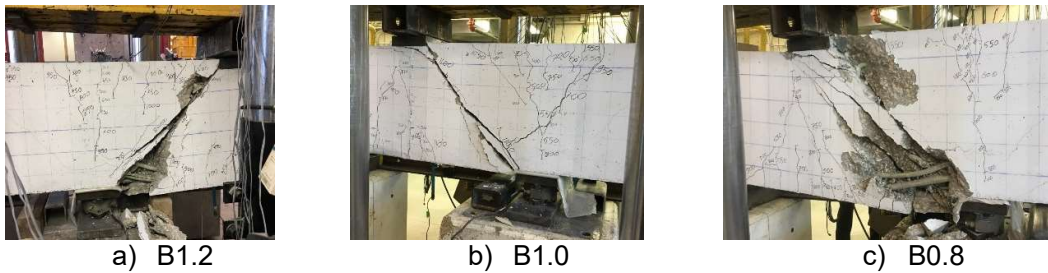


Figure 3: Failure Modes

**Load capacity**

This study shows that decreasing the  $\rho_t$  has a great influence on the load capacity of continuous deep beams reinforced with GFRP as shown in Figure 4. Test results show that decreasing  $\rho_t$  from 1.2 to 1.0 resulted in increasing in the load capacity by 30%, similarly an increase of 37% of the load capacity was observed with decreasing  $\rho_t$  from 1.0 to 0.8. The enhancement in the load capacity is attributed to the redistribution of the internal forces that was enhanced by reducing the stiffness of the top reinforcement (tie).

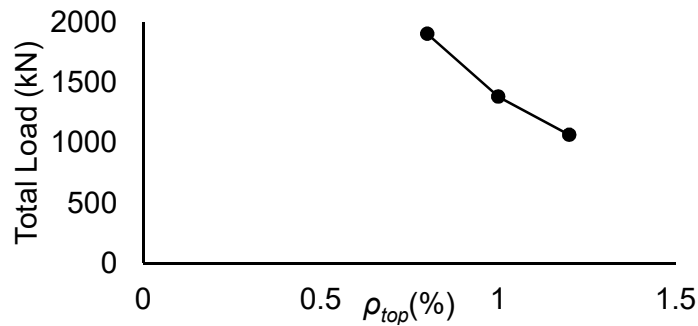


Figure 4: Load capacity versus longitudinal top reinforcement ratio.

## Strains in reinforcement

Figure 5 shows the reinforcement strain distribution for specimen B0.8. Generally, the developed strains in the reinforcement were very small until the formation of the flexural cracks, at hogging zone then sagging zone, a rapid increase in the strain at the location of the flexural cracks representing the bending moment of such loading case. With further loading, the development of strains increased along the bar length confirming the formation of the STM and tended to be similar along the bar length.

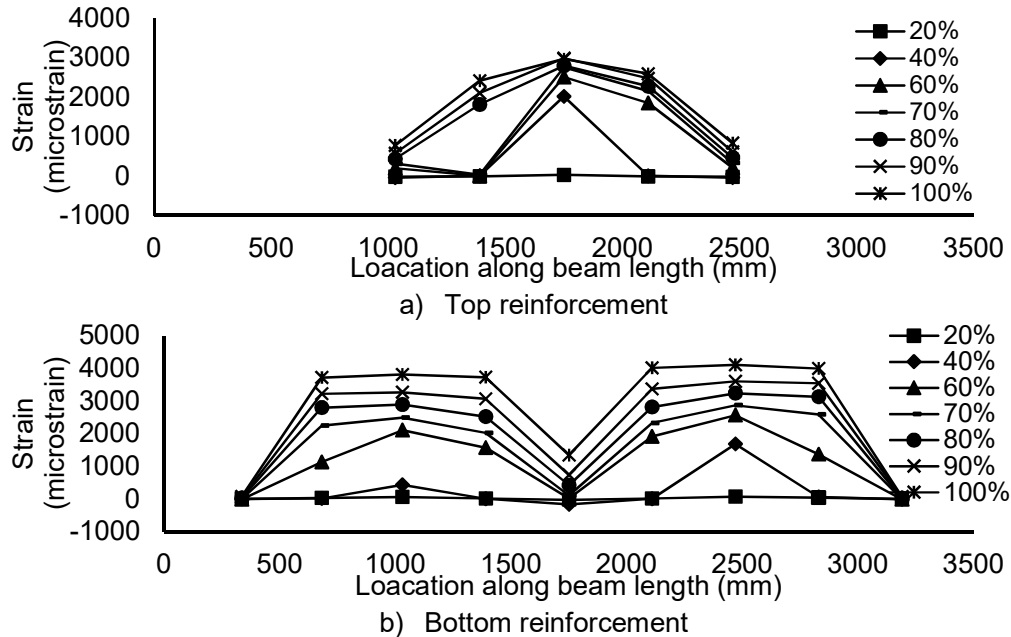


Figure 5: Strain profile of specimen B0.8

## Conclusions

Based on the presented discussions, the following can be concluded:

1. Failure of all specimens was brittle. All specimens failed after the formation of a major diagonal shear crack extending from the inside edge of the middle support plate toward the loading plate.
2. An arch mechanism formed in all specimens. This was confirmed by the crack orientations and measured strains in the longitudinal reinforcement.
3. The load capacity of the specimens increased as the  $\rho_{top}$  ratio increased.

## References

- [1] ACI Committee 440.1R, 2015. "Guide for the Design and Construction of Structural Concrete Reinforced with FRP Bars." ACI 440.1R-15, American Concrete Institute, Detroit, MI, USA, pp. 1-88.
- [2] ISIS Canada, 2007. "Reinforcing Concrete Structures with Fibre Reinforced Polymers". Winnipeg, Manitoba, Canada, pp. 1-151.
- [3] ASCE-ACI Committee 426, 1973. "Shear and Diagonal Tension.". ASCE, Journal of Structure Division, (6), pp. 1091–1187.
- [4] Wight, J. K. and MacGregor, J. G., 2009. "Reinforced Concrete: Mechanics and Design." (6th edition), Pearson Prentice Hall, Upper Saddle River, New Jersey, USA, pp. 1-1157.
- [5] Razaqpur, G. A., Isgor, B., Greenaway, S., and Selley, A., 2004. "Concrete contribution

- to the shear resistance of fiber reinforced polymer reinforced concrete members." *J. Compos. Constr.*, 10.1061/(ASCE) 1090-0268(2004)8:5(452), pp. 452–460.
- [6] Manuel, R., Slight, B., and Suter, G., 1971. "Deep Beam Behavior Affected by Length and Shear Span Variations." *ACI Journal Proceedings*, 68(12), pp. 954–958.
- [7] Rogowsky, D. M., MacGregor, J. G., and Ong, S. Y., 1986. "Design of Reinforced Concrete Deep Beams." *ACI Journal Proceedings*, 83(4), pp. 614–623.
- [8] Ashour, A. F., 1997. "Tests of Reinforced Concrete Continuous Deep Beams." *ACI Structural Journal*, 94(1), pp. 3–11.
- [9] Yang, K. H., and Ashour, A. F., 2007. "Influence of Section Depth on the Structural Behaviour of Reinforced Concrete Continuous Deep Beams." *Magazine of Concrete Research*, 59(8), pp. 575–586.